International Journal of Advanced Geosciences, 14 (2) (2026) 124-137

International Journal of Advanced Geosciences

Website: www.sciencepubco.com/index.php/IJAG
https://doi.org/10.14419/pe1ksz87
Research paper

Geospatial Mineral Prospectivity Mapping Using Multi-Source Remote Sensing and AHP-Based Analysis in Bapatla District, Andhra Pradesh, India

Sreerama Naik S. R. *, T. K. Prasad, Jayapal G.

Department of Geography, SAT Campus, Kannur University, Payyanur, Kerala. India
**Corresponding author E-mail: rs_sreeramanaik@kannuruniv.ac.in*

Received: 7 Sep 2026, Accepted: 10 Nov 2026, Published: 20 Nov 2026

Abstract

The mineral prospectivity mapping approach can be utilised for exploring and prioritising mineralisation sites with the aid of geological, structural, spectral and terrain-based evidence. The current study performed mineral prospectivity analysis of Bapatla district, Andhra Pradesh, India, using a multi-thematic geospatial and remote sensing approach. The study is framed as a preliminary screening of any spectral and structural anomalies for coastal/alluvial heavy mineral or lateritic iron concentrations and structurally controlled basement-hosted mineralisation in the northwestern interior. The relief, slope and Topographic Position Index were derived to understand the geomorphology of the region. Drainage density and lineament density aided in demarcating structural geomorphology and zones of fluid flow that may host mineral deposits. An AHP weighted overlay of eight layers, including lineament density, an alteration-related spectral index, clay mineral index, iron oxide index, drainage density, slope, Bare Soil Index and NDVI, was used to calculate a relative spectral–structural prospectivity index; Ferric Iron, Ferrous Mineral, Quartz, NDMI, relief, TPI and PC4 were mapped as auxiliary information. Spectral indices were calculated after masking out vegetated and/or moist/wet pixels. Most of the area in the study region was found to have Very Low to Medium mineral prospectivity, whereas High and Very High prospectivity were restricted to narrow structural zones. The study revealed three zones of relatively higher index values in the northwestern Addanki-Martur-Ballikurava region, central Parchur-Karamchedu-Bapatla region and coastal Chinaganjam-Nizampatnam-Repalle region. Principal Component Analysis of six of the Sentinel-2 bands was used to investigate spectral variability. The eigenvector loadings of PC4 are reported to test whether it relates to an alteration-related contrast. A qualitative comparison with a mineral occurrence map indicated that only broad spatial agreements were present. No quantitative evaluation, such as ROC/AUC or prediction–area analysis, is given. The outputs provide a first screening of potential spectral and structural anomalies for field verification and should not be considered as confirmed mineralised zones.

Keywords: *Mineral Prospectivity Mapping; Remote Sensing; GIS; Spectral Mineral Indices; Principal Component Analysis; Bapatla District.*

1. Introduction

Mineral resources underpin industrial development, so recognising areas where they may occur is the primary objective of exploration geology (Bonham-Carter, 1994; Carranza, 2008). Field surveys, drilling, and geochemical sampling are time-consuming and often infeasible at regional scale. Exploration geology has benefited immensely from advances in satellite remote sensing (RS) and geographic information systems (GIS) in recent decades, enabling rapid, repeated acquisition of spatial information on lithology, tectonics, and surficial mineralogy (Gupta, 2003; Bhatta, 2008). Notably, multispectral and hyperspectral RS sensors enable identification of diagnostic spectral absorption bands of hydrothermally altered minerals associated with ore-forming processes (Van der Meer et al., 2012).

Since their first use in the Cuprite mining district, Nevada, to distinguish hydrothermally altered, mineralised rocks from unaltered country rocks using computer-assisted multispectral imagery (Abrams et al., 1977; Rowan et al., 2003), remote sensing technologies have played a critical role in regional reconnaissance mineral exploration. The Advanced Spaceborne Thermal Emission and Reflection Radiometer (ASTER) shortwave and thermal infrared bands have been used to identify clay, mica, carbonate, and silicate minerals (Abrams, 2000; Yamaguchi & Naito, 2003; Ninomiya et al., 2005). Band ratioing, first proposed to identify alteration mineral assemblages, remains a popular technique for minimising topographic effects while highlighting subtle differences in the spectral properties of altered and unaltered lithologies (Sabins, 1999).

Principal component analysis (PCA) is a powerful technique widely used in mineral prospectivity analysis to identify spectral regions in multispectral imagery associated with occurrences of hydroxyl and iron-oxide alteration minerals (Crosta & Moore, 1989; Loughlin, 1991). The 4th PC, which is diagnostic of argillic and phyllic alteration mineral assemblages, has been used as a key evidential layer in mineral prospectivity analysis of porphyry Cu deposits in NE Iran (Tangestani & Moore, 2002) and epithermal Au deposits in NW Argentina (Crosta et al., 2003). Hydroxyl clay mineral abundance and iron oxide mineral abundance are two other key evidential layers in mineral prospectivity analysis. The former utilises absorption features in the visible to shortwave-infrared spectrum to estimate hydroxyl clay

Copyright © Sreerama Naik S. R., T. K. Prasad and Jayapal G. This is an open access article distributed under the Creative Commons Attribution License, which permits unrestricted use, distribution, and reproduction in any medium, provided the original work is properly cited.

abundance using the clay mineral index, while the latter uses diagnostic absorption features of ferric and ferrous oxides to estimate iron oxide mineral content as an indicator of hydrothermal alteration (Gad & Kusky, 2006). These features serve as indicators of hydrothermal fluid–rock interactions and have been linked to mineralisation processes.

Hydrothermal mineralisation occurs in fractured lithologic settings, so lineament density estimates derived from digital elevation models (DEMs) provide valuable insights into the structural controls on mineralisation. Lineament density has been shown to correlate with the degree of fracturing in a given area, which in turn governs the hydrodynamic potential and structural complexity required to host significant mineral deposits (Hung et al., 2005; Abdullah et al., 2010; Manyoe & Hutagalung, 2021; Nugroho & Tjahjaningsih, 2016). By contrast, drainage density and slope serve as surrogates for lithology, structural grain, and weathering potential (Bonham-Carter et al., 1989; Arulbalaji et al., 2019). The bare soil index, derived from the optical bands, is another useful indicator of regolith cover thickness and has been used extensively in tropical environments to identify areas under vegetation cover where hydrothermal alteration and mineralisation may be masked (Behnia et al., 2012).

Each of these evidential layers can be combined using a multi-criteria decision analysis framework to generate a mineral prospectivity map, with the choice of the best method dictated by the nature of available data and the study's geological context. The analytic hierarchy process (AHP) decision-making methodology is one such approach that has been widely used in exploration geology. It is a knowledge-based multi-criteria decision analysis method that relies on pairwise comparisons of the input criteria to derive a set of criterion weights following Saaty's eigenvector method (Saaty, 1980; fuzzy extensions: Chang, 1996). The consistency ratio of criterion weights can be evaluated using the same methodology, giving an option to quantify the level of consistency that needs to be achieved at each level of the decision-making hierarchy (Saaty, 1980).

AHP and related knowledge-driven approaches have been used in mineral prospectivity modelling of gold systems (Carranza & Hale, 2001; Behera et al., 2019; Carranza et al., 2015), as well as in groundwater potential assessment using lineament density, drainage density, slope, and geomorphology (Arulbalaji et al., 2019). A review of mineral prospectivity modelling studies by Yousefi et al. (2021) highlights the importance of knowledge-based modelling in complementing data-driven and machine learning methods in areas where there is limited field mineral occurrence data available. Recent studies have added hyperspectral imagery (Hajaj et al., 2024), machine learning algorithms (Guo et al., 2023), and remote sensing and spatial prediction of lithology (Behnia et al., 2012) to the list of potential evidential layers in mineral prospectivity analysis. Regional studies from Morocco (Benaissi et al., 2022), Tibet (Fu et al., 2023), Iran (Maleki et al., 2021) and central India (Behera et al., 2019) highlight the application of mineral prospectivity studies using a combination of RS and GIS methods.

An important aspect of mineral prospectivity analysis is the recognition of mineral systems, in which a combination of a source for mineralisation, a mechanism to transport it to a repository, and the repository itself all play a role in deposit formation (McCuaig et al., 2010). This concept provides the theoretical basis for combining the various evidential layers from structural geology, lithology, and hydrothermal alteration to predict potential areas of mineralisation. There is a paucity of studies that combine these evidential layers using the AHP decision support methodology.

While mineral prospectivity modelling has been conducted extensively in mineral-endowed jurisdictions around the world, the application of this framework to coastal, cratonal geology is limited. This study attempts to bridge this gap by applying a knowledge-driven AHP-based weighted overlay to the Bapatla district, Andhra Pradesh, located on the border between the Eastern Ghats mobile belt and the Krishna-Godavari coastal tract. This district has an underdeveloped exploration history, and the study aims to contribute towards filling this gap. Because the district is largely composed of Quaternary alluvial and coastal deposits with only a few places of outcrops of crystalline rocks, the findings are considered an initial screening of spectral and structural anomalies for a potential mineral deposit type. Specifically, this study will:

1) Derive lineament density, drainage density, slope, bare soil index, NDVI and clay-mineral, iron-oxide and alteration-related spectral indices (PC4, quartz, ferric and ferrous iron, NDMI, relief and TPI as supportive layers) from remote sensing and GIS data;
2) To apply Saaty's pairwise-comparison AHP to weight the eight evidential layers, report the consistency of the judgements (CI and CR) and generate a relative prospectivity index map; and
3) To evaluate the map by comparing it with the mineral occurrence data using ROC/AUC and prediction–area analysis.

1.1. Data

The identification of mineral prospecting zones is a complex task, which requires the analysis of various spatial data. In this research, a mineral prospectivity index was constructed using the remote sensing data obtained via satellites. The data were analysed using the GIS-based MCDA method, using the weighted linear combination of the thematic layers. The AHP approach was used to estimate the weights of the different factors that contribute to mineralisation. The final prospectivity map was validated with the known mineral locations.

Acquisition details. Sentinel-2A Level-2 surface-reflectance scenes were filtered from a dry-season, post-harvest window with <5% cloud cover, cloud- and shadow-masked using SCL, and reduced to a composite; B2, B3, B4, B8, B11, and B12 were used (B11/B12 resampled to 10 m). Sentinel-1 GRD scenes were acquired in IW mode; the Carto-DEM is 30 m. The ASTER product used has a resolution of 30 m. Acquisition dates and season matter because crop cover and soil moisture change the SWIR response of agricultural soils.

Table 1: Data Sources Used in the Study.

Sl. No.	Data	Source	Spatial Resolution	Purpose
1	Sentinel-2A MSI Level-2	Copernicus European Space Agency (ESA)	10 m	Spectral Mineral Indices, NDVI, NDMI, BSI and PCA
2	Sentinel-1 Ground Range Detected (GRD)	Copernicus European Space Agency (ESA)	10 m	Lineament and Structural Analysis
3	Carto-DEM	Bhuvan Portal	30 m	Slope, Relief and TPI
4	Carto-DEM	Bhuvan Portal	30 m	Stream Extraction and Drainage Density
5	ASTER	NASA/USGS	[30 m SWIR]	Land-surface temperature context
6	Geological layers	NGDR	1:25,000	Lithology, faults and mineral occurrences
7	Lithology	GSI	1:25,000	Lithological Boundaries
8	Soil Map	NBSS & LUP	1:25,000	Bare Soil
9	Google Earth Engine Catalogue	Google Earth Engine	Cloud Platform	Data processing, analysis, and export

1.2. Methodology

Data acquisition involved downloading various datasets from databases (Table 1). The Sentinel-2A MSI Level-2 products (10 m) were used to calculate the mineral indices such as Iron Oxide, Clay Minerals, an alteration-related (hydroxyl) index, Quartz, Ferric Iron, and Ferrous Minerals, and vegetation indices like NDVI, NDMI, and Bare Soil Index from the Copernicus programme of the European Space Agency (ESA). Sentinel-1 GRD products from the Copernicus programme were used to extract the lineaments from the study area and delineate the lithostructural geology. The Carto-DEM (30 m) was downloaded from the Bhuvan portal to estimate morphological features like slope and relief, Topographic Position Index (TPI), and drainage density and pattern. The ASTER thermal band was used to estimate land-surface temperature; surface temperature is not an indicator of hydrothermal alteration. The thematic layers such as lithology and structural features were downloaded from the National Geoscience Data Repository (NGDR) and the National Bureau of Soil Survey and Land Use Planning (NBSS&LUP), respectively, at a 1:25,000 scale. Similarly, lineaments were extracted from the Bhuvan portal at a 1:25,000 scale, and all datasets were pre-processed in GEE for further analysis.

Index definitions and lineament source: The band-ratio definition of each spectral index, namely, clay, iron oxide, ferric iron, ferrous mineral, alteration-related, and quartz. The lineament source is based on GSI mapping; it may not be independent of the NGDR occurrence layer used for validation.

Terminology: In this paper, the 'Hydrothermal Alteration Index' refers to a spectral band-ratio index which is responsive to hydroxyl- or oxide-bearing minerals and the high values of which indicate regions of spectral anomaly rather than hydrothermal alteration, which would require petrographic or geochemical identification. The term 'thermal' alteration is not used; the ASTER thermal data only record land-surface temperature.

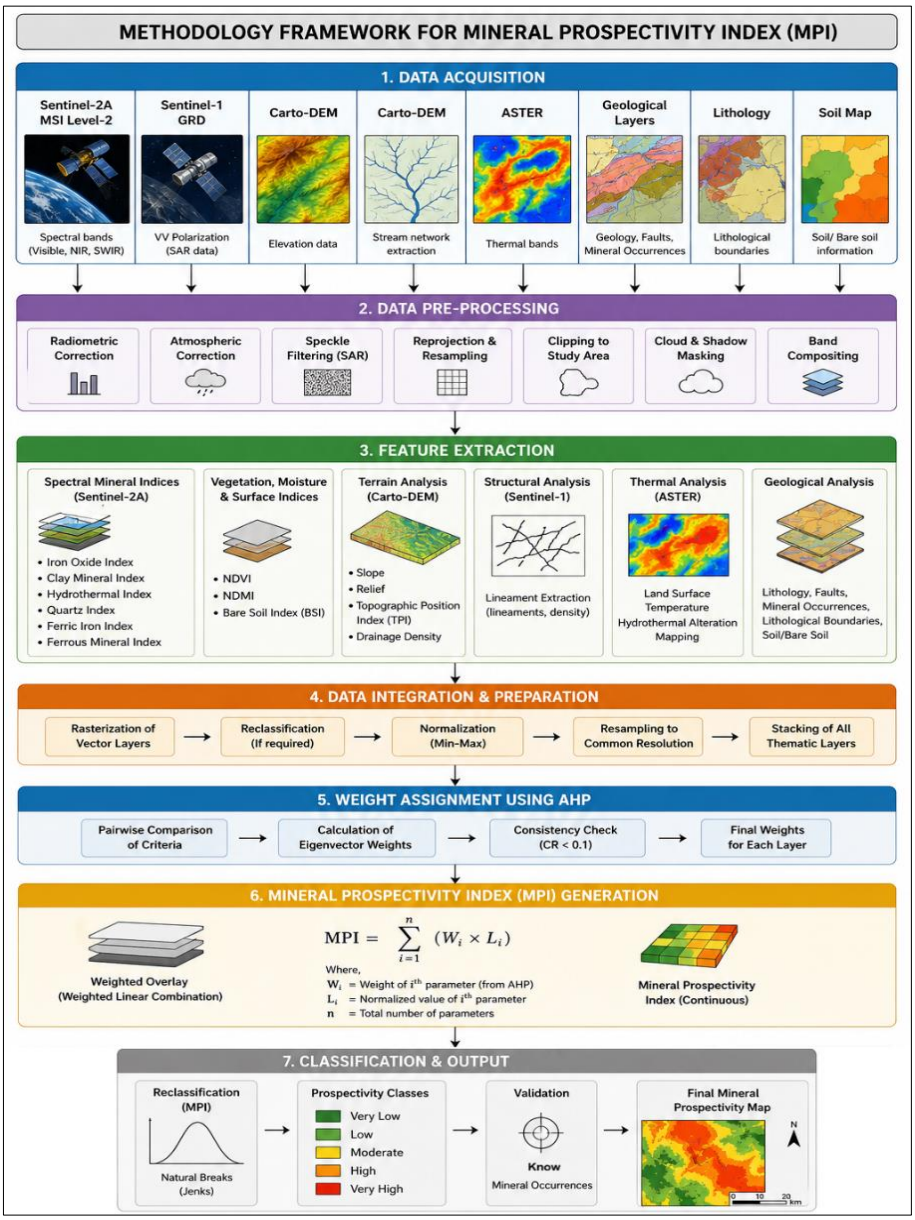


Fig. 1: Flow Chart of the Methodology.

The process involved radiometric and atmospheric corrections, SAR speckle noise reduction, reprojection, clipping, and resampling of all raster datasets to a suitable reference system, cloud masking, and other preprocessing steps. The vector datasets were converted to raster data, clipped, and merged with the raster dataset for further processing. After pre-processing, feature extraction procedures were performed to generate thematic indicator classes for different controls on mineral occurrences and prospectivity assessment. The thematic classes include mineral indices, vegetation indices, bare soil index, morphological features, drainage density, land-surface temperature, lineament

density, and others. The extracted thematic classes were rasterised and standardised using min-max scaling, reclassified as necessary, resampled to a uniform resolution, and then combined into a stack of raster images. AHP was used to assign weights to each thematic class based on the Eigenvalue and Consistency Ratio (CR). The pairwise comparison matrix was made, and the eigenvector of the matrix was evaluated, and a consistency ratio was estimated to be less than 0.1, thus indicating that the judgments made were consistent.
Masking of vegetated and moist pixels: The district consists mostly of cropland, irrigated land, and coastal wetland, and SWIR-based band ratios on vegetated or moist surfaces produce false anomalies (Carranza & Hale, 2002). Before calculating the spectral mineral indices, pixels had to be masked, as was done for the calculation of the NDVI, NDMI and BSI, which were used as masks and indicators of quality; if NDVI was also included in the weighted sum, the direction of the score would be inverted (higher score for lower NDVI). All the spectral mineral abundance maps, the MPI, and Table 4 had to be recalculated after masking.
The weighted overlay analysis is achieved by multiplying the normalised attribute values and their corresponding weights to arrive at a mineral prospectivity index (MPI) represented by the equation:

$$MPI = \Sigma (Wi \times Li)$$

Where
Wi = Weights assigned to each parameter based on the AHP.
Li = Normalised values of the ith parameter
The resulting continuous surface of MPI was classified into five classes using Jenks breaks (Natural breaks) classification. The classes were assigned labels in the following order from low to high: Very Low, Low, Moderate, High, and Very High.

1.3. Analytical hierarchy process (AHP)

The Analytical Hierarchy Process (AHP) was used as a multi-criteria decision analysis approach to merge the normalised thematic layers through the calculation of the Mineral Prospectivity Index (MPI). Weights were assigned to each thematic layer on the basis of their relative importance or influence on the presence of minerals. The weights were derived from expert judgement and geological reasoning; expressed as an 8 × 8 pairwise-comparison matrix on Saaty's 1–9 scale (Table 3). The eight thematic variables entering the weighted overlay are listed in Table 2. Ferric Iron, Ferrous Mineral, Quartz Index, NDMI, relief, TPI and PC4 were derived as supporting layers for interpretation and are not part of the weighted sum.

Table 2: AHP Weights of the Eight Evidential Layers (Sum = 1.00)

Sl. No.	Parameter	Weight
1	Lineament Density	0.25
2	Alteration-related Spectral Index	0.20
3	Clay Mineral Index	0.15
4	Iron Oxide Index	0.15
5	Drainage Density	0.10
6	Slope	0.05
7	Bare Soil Index (BSI)	0.05
8	NDVI	0.05

Table 3: AHP Pairwise-Comparison Matrix (Saaty 1–9 Scale), Principal Eigenvector, Λmax = 8.06, CI = 0.0088, RI = 1.41 (N = 8), CR = 0.006 (< 0.10)

	LD	HA	CM	IO	DD	S	BSI	NDVI
LD	1	1	2	2	2	5	5	5
HA	1	1	1	1	2	4	4	4
CM	1/2	1	1	1	1	3	3	3
IO	1/2	1	1	1	1	3	3	3
DD	1/2	1/2	1	1	1	2	2	2
S	1/5	1/4	1/3	1/3	1/2	1	1	1
BSI	1/5	1/4	1/3	1/3	1/2	1	1	1
NDVI	1/5	1/4	1/3	1/3	1/2	1	1	1

All themes were normalised using min – max transformation to make a set of dimensionless data that ranged from 0 to 1. Based on these normalised values, we calculated the mineral prospectivity index for each cell using the linear combination function, which was given below:

$$MPI = (0.25\times LD)+(0.20\times HA)+(0.15\times CM)+(0.15\times IO)+(0.10\times DD)+(0.05\times S)+(0.05\times BSI)+(0.05\times NDVI)$$

Where:
- LD = Lineament Density
- HA = Alteration-related Spectral Index (spectral proxy for hydroxyl/iron-bearing minerals)
- CM = Clay Mineral Index
- IO = Iron Oxide Index
- DD = Drainage Density
- S = Slope
- NDVI = Normalised Difference Vegetation Index
- BSI = Bare Soil Index

The equation uses the same eight layers, in the same order and with the same weights, as Table 2; the weights sum to 1.00. Supporting layers are not part of the equation.

1.4. Principal component analysis (PCA)

Principal Component Analysis was applied to reduce the dimensionality of highly correlated multispectral Sentinel-2 bands and to enhance the lithology and hydrothermal alteration information while minimising the amount of information overlapping with redundant spectral

bands. The six spectral bands of Sentinel-2, including Blue-B2, Green-B3, Red-B4, Near Infrared-B8, Shortwave Infrared-1 B11, and Shortwave Infrared-2 B12, were used as initial inputs for PCA. First, for each pixel, a mean spectral value was estimated for the given area and centred by subtracting the mean value for each band. Then, using centred images, a covariance matrix was calculated, based on which eigenvectors and eigenvalues were estimated to identify the main directions of variability in the dataset. As a result, six principal components (PC1–PC6) were extracted from the study-area pixels. These components contain independent information in decreasing order of spectral variance. PC4 was provisionally selected as a candidate alteration-related layer based on feature-oriented PCA (Crosta & Moore, 1989; Loughlin, 1991), and is accepted only if its eigenvector loadings show a diagnostic contrast: (i) opposite-sign loadings of B11 (SWIR-1) and B12 (SWIR-2) for hydroxyl/clay minerals, or (ii) opposite-sign loadings of B2 (blue) and B4 (red) for iron oxides. If PC4 fails to show such a contrast, or is dominated by the loading of B8 (vegetation), it is treated as noise or land-cover variance, and not evidence of argillic or phyllic alteration. PC4 was then normalised to the 0-1 range, with other theme layers being used in prospectivity analysis. Since all six components were retained, there was no dimensionality reduction; PCA was used here to explore spectral structure, and to isolate out of these, PC4, which is a supporting layer and not part of the MPI.

2. Study Area

The study was conducted in Bapatla District, central coastal Andhra Pradesh, India. This district is located in the coastal plain of Andhra Pradesh and is characterised by relatively flat topography, alluvial sediments, a network of irrigation canals and drains, ponds, lakes, and fertile agricultural lands. The district is located between 15°54′ and 16°19′ N latitude and 80°00′ and 80°51′ E longitude in the coastal region of the Bay of Bengal. Bapatla District covers an area of 3,829 km 2 and consists of 25 mandals spread over three revenue divisions: Bapatla, Chirala, and Repalle. The coastal district of Bapatla is bounded on the east by the Bay of Bengal, while the alluvial sediments of the delta plain dominate the interior. The surface is generally gently sloping, ranging from approximately mean sea level along the coast to about 20-40 m above mean sea level inland. There is a gentle slope towards the southeast direction facilitating drainage into the Bay of Bengal, resulting in waterlogged areas during heavy rainfall and cyclones.

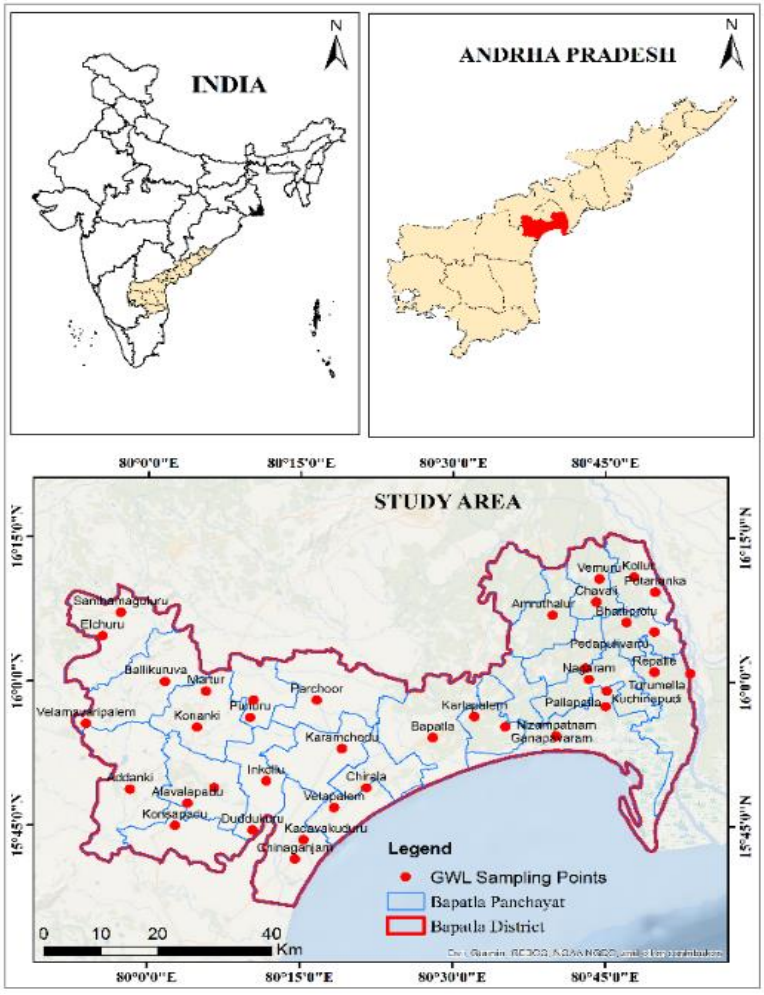


Fig. 2: Location Map of the Study Area.

Bapatla District has a tropical monsoon climate, with rainfall mainly occurring during the southwest monsoon season (June-September) and partly during the northeast monsoon and the cyclones originating from the Bay of Bengal. In addition, the coastal tract of the district is vulnerable to periodic cyclones and heavy rains, causing widespread inundation of the agricultural lands. The main crops include paddy, pulses, cotton, chilli, vegetables, and maize. Apart from canal irrigation and bore wells, aquaculture and inland fisheries are also significant contributors to the state's economy. Groundwater plays a significant role in irrigation and drinking water in the region. The geology of the district consists mainly of Quaternary sediments of alluvial and coastal deposits, with some crystalline rocks occurring in the interior parts of the district. Groundwater flow systems are controlled by the distribution of different rock types. However, the coastal aquifers undergo

anthropogenic stresses such as over-exploitation, urbanisation, and saline water intrusion. Bapatla is a suitable study area due to its geographical location, sloping plain alluvial tract with a network of drainage canals, agriculture, and groundwater dependence. It will provide a good basis to evaluate the relationship between the geomorphology, spectral mineral signature, and mineral prospectivity of a region.
Geological setting: The district lies between the Eastern Ghats mobile belt and the Krishna-Godavari coastal tract [authors to specify the basement lithologies, structural trends and any known mineral showings from the GSI district resource map and quadrangle reports, with citations]. Surface exposure is dominated by Quaternary alluvial, deltaic and coastal sediments, with crystalline rocks and lateritic cover only exposed in the interior [confirm]. Most spectral signals in the district, therefore, originate from alluvial soils, cropland and coastal sands rather than from exposed bedrock.
Target mineral system: The study does not target a single confirmed deposit type. Two possible targets in this setting are [authors to select and justify]: (i) surficial or placer-type systems, i.e. heavy-mineral or iron-rich (lateritic) accumulations in coastal and alluvial sediments, in which the mineral-system components are a crystalline or lateritic source terrane, fluvial or coastal transport, and a depositional trap; and (ii) structurally controlled, basement-hosted mineralisation in the north-western interior, where fractures act as fluid pathways and clay/iron oxide spectral signals act as a proxy for alteration. In this framework, lineament and drainage density are proxies for structural permeability through thin cover, the iron oxide and clay indices respond to ferric-iron-bearing and clay-rich surface material, and slope and relief indicate where bedrock or laterite may outcrop. These surface signals can only be linked to subsurface ore-forming processes after field and geochemical confirmation; until then, they are interpreted as spectral anomaly zones.

3. Result and Discussion

3.1. Terrain

Bapatla District is located on the Andhra Pradesh coast; thus, it is largely located in the Krishna-Guntur coastal plain. The region is expected to have a relief of low and gently undulating alluvial and deltaic plains, except for slightly higher ground inland in the district's northwest. The three derivative terrain maps below (Relief, Slope, and Topographic Position Index) highlight some differences in land relief. The first one is dominated by lowlands, with few places of high, steep topography; the second one is also dominated by lowlands with some gentle slopes; the third one illustrates the general flatness of most lowlands and the few places with crest/slope.

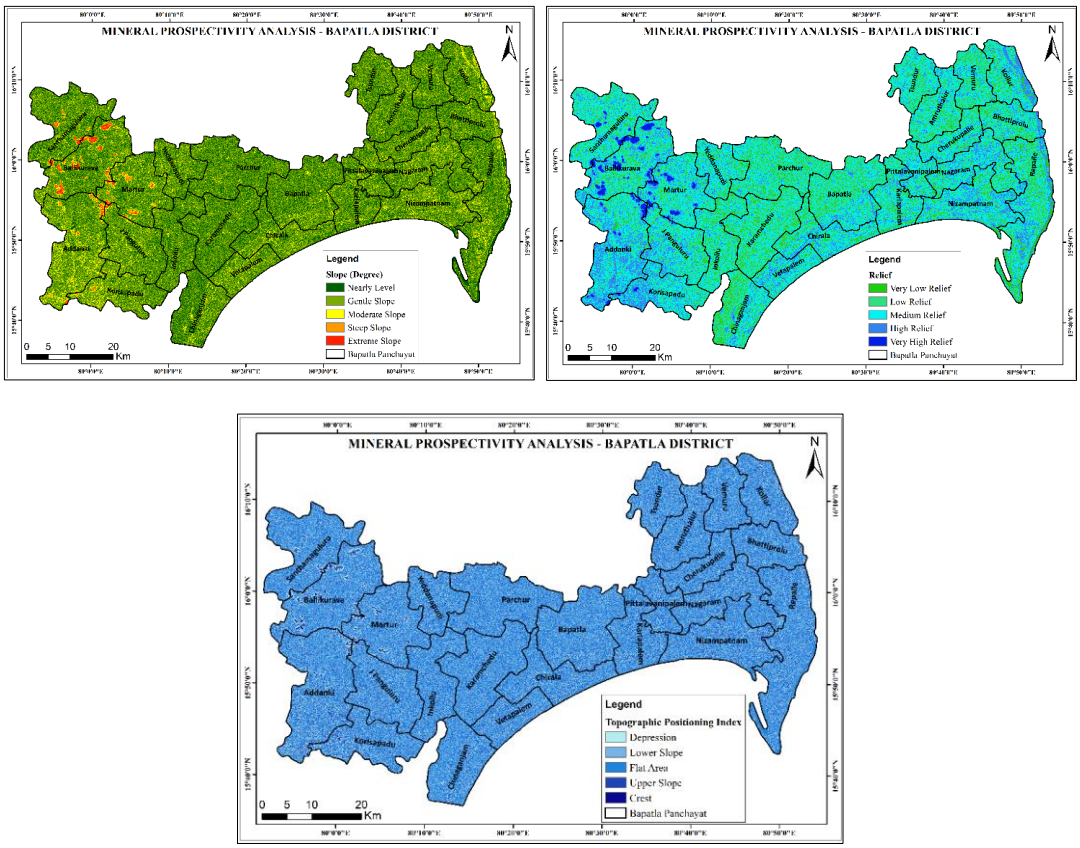


Fig. 3: Terrain Derivatives of Bapatla District: Relief, Slope and Topographic Position Index.

3.1.1. Slope

The slope map shows some similar patterns in the lowlands of coastal Andhra. Nearly all of the Bapatla district (all mandals) are dominated by Nearly Level to Gentle Slopes. Only a handful of pixels across the region have Moderate Slopes. This gives the Slope map the same "salt-and-pepper" appearance as the previous map. Most areas with Steep to Extreme Slopes are found in the Santhamaguluru, Martur, Ballikurava belt in the northwest. Therefore, the patterns of the slope map are generally similar to those observed on the relief map. In particular, there are a few areas with steep slopes in the northwest, while most other areas have gentle slopes or are nearly level.

3.1.2. Relief

Overall, the relief map shows that most of the district (all mandals) are dominated by Medium Relief. This includes most of the coastal (inland) mandals of Bapatla district, which are generally flat deltaic plains with minor topographic fluctuations. Some of the mandals (Nizampatnam, Repalle, Chirala) in the eastern coastal area also exhibit Medium Relief, but they are generally Low. At the same time, the Santhamaguluru, Ballikurava, Martur, and Kottapalle mandals in the northwest are characterised by isolated High and Very High Relief (dark blue areas), which suggests that this area has some higher ground or rocky outcrops that are not typical for the lowlands of coastal Andhra.

3.1.3. Topographic positioning index

Most of the area (all coastal areas) falls under the Flat Area class of the TPI map. There were only a handful of pixels with Lower Slope and Upper Slope/Crest in the Santhamaguluru-Martur-Ballikurava belt in the northwest. Hence, similar to the previous two maps, there are only a few areas in the Bapatla district with slope crests or depressions. There were virtually no pixels with the Depression class. Overall, the TPI map suggests that most of the Bapatla district is a lowland with little variation in terrain elevation. However, the Santhamaguluru-Martur-Ballikurava belt in the northwest appears to have a few isolated higher ground areas. This information corroborates the findings of the previous two maps – the Bapatla District is generally a lowland with little variation in elevation. Therefore, any potential mineral prospecting areas would be limited to the northwest areas of the district.

3.2. Structural

Beyond the surface-form parameters of relief, slope, and terrain position, structural indicators such as drainage texture and lineament pattern reveal how subsurface geology, fracturing, and hydrological development have shaped Bapatla District, factors that are directly relevant to groundwater movement, weathering, and the structural conduits that can host mineralisation. The Drainage Density and Lineament Density maps below capture these structural controls, showing how the district's near-flat coastal setting still preserves meaningful variation in stream network development and fracture-related linear features.

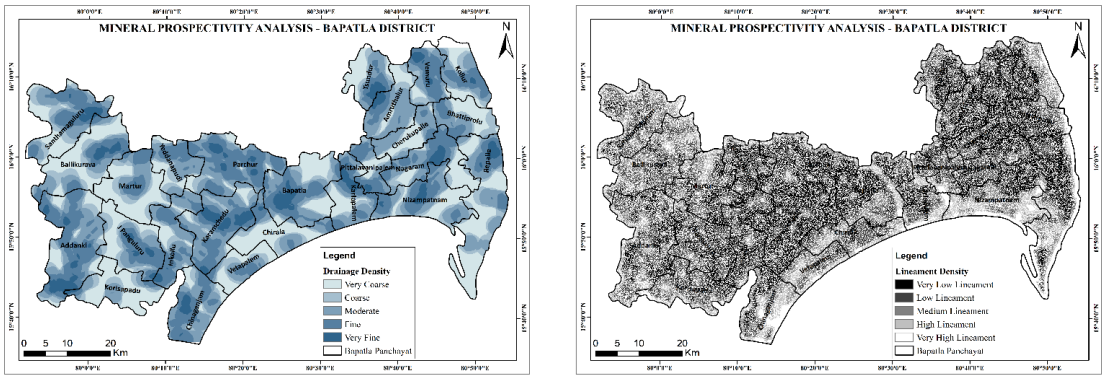


Fig. 4: Structural Layers: Drainage Density and Lineament Density.

3.2.1. Drainage density

The drainage density map shows a mosaic dominated by Very Coarse to Moderate classes across most of the district, consistent with the low-relief, gently sloping coastal plain that limits the development of dense stream networks. However, numerous discrete patches of Fine and Very Fine drainage density are distributed throughout almost every mandal, including Bapatla, Karamchedu, Parchur, Martur, Addanki, J Panguluru, Chinaganjam, and the northeastern cluster around Amruthalur, Cherukupalle, and Bhattiprolu, indicating localised zones of more closely spaced stream channels. These fine-drainage nodes typically coincide with slightly elevated or structurally disturbed ground where surface runoff is channelled more efficiently, and their clustering near settlement centres and mandal boundaries suggests a correlation with subtle lithological or structural discontinuities rather than a purely random distribution, making them useful indicators for zones of enhanced permeability or fracture-controlled drainage development.

3.2.2. Lineament density

The lineament density map, rendered in a grayscale texture from Very Low to Very High lineament concentration, shows that most of the district falls into the Low to Medium Lineament classes, forming a fairly uniform mottled grey fabric typical of alluvial cover where surface fracture traces are subdued by sediment overburden. Nonetheless, the eastern and northeastern mandals Repalle, Nizampatnam, Bhattiprolu, Cherukupalle, Amruthalur, Vemuru, and Kollur display a visibly higher concentration of Medium to High Lineament density, suggesting a structurally more fractured or faulted terrain in this coastal-to-near-coastal belt, possibly linked to the influence of the Krishna River delta margin and associated tectonic lineaments. In contrast, the western mandals such as Addanki, Korisapadu, and Santhamaguluru show a comparatively lower and more uniform lineament density, reinforcing that structural fracturing is not evenly distributed and that the north-eastern zone, alongside the northwestern high-relief pocket identified earlier, represents a structurally significant sector where lineament intersections and drainage anomalies together could mark favourable corridors for mineral-bearing fluid pathways or fracture-hosted deposits. Many lineaments are actually the result of natural landforms or manmade structures such as canals, drains, embankments, roads, and field boundaries. The lineament layer should be masked with these cultural features. Lineament density is thus interpreted as a structural indicator of uncertain geology.

3.3. Spectral mineral indices

Spectral mineral indices, obtained through the ratio of bands, identify the mineral compositions by their spectral absorption and reflectance properties, and consequently, they highlight the areas of clay mineralisation, iron content, hydrothermal alteration, and silica enrichment

in Bapatla District for mineral prospectivity assessment. The six mineral indices (i.e., Clay Mineral, Ferric Iron, Ferrous Mineral, Hydrothermal Alteration, Iron Oxide, Quartz Index) delineate the regions with anomalous traces of specific minerals, with the intersecting areas suggesting the possible zones with prospectivity. These indices are considered as spectral anomalies. In this context, they can represent soil colour, water content, agricultural land use, and mineralogy of sediment and bedrock or laterite, which are calculated on the pixels remaining after the vegetation and moisture masking.

3.3.1. Clay mineral

The clay mineralisation map indicates that the majority of the area is characterised by Low/Intermediate levels of clay minerals, whereas Medium levels occupy the central-eastern part of the district, including Bapatla, Karlapalem, Pittalavanipalem, coastal mandals of Nizampatnam, and Repalle. One particular region of interest is the relatively isolated patch of Very High (dark olive) level in the coastal vicinity of Repalle, which stands out as a zone of strong clay mineralisation, compared to the overall Low/Moderate background of most of the district.

3.3.2. Ferric iron

As the next mineral composition, Ferric Iron is also found in High and Very High concentrations throughout the territory, with a noticeable focus on the district's NE part (Tsundur, Amruthalur, Vemuru, Kollur, Cherukupalle, Bhattiprolu) as well as scattered spots in central (Parchur, Karamchedu, Ballikurava) and western (Santhamaguluru, Martur, Yeddanapudi) mandals. Meanwhile, the coastal edge of Nizampatnam and Repalle is covered with low-ferric iron.

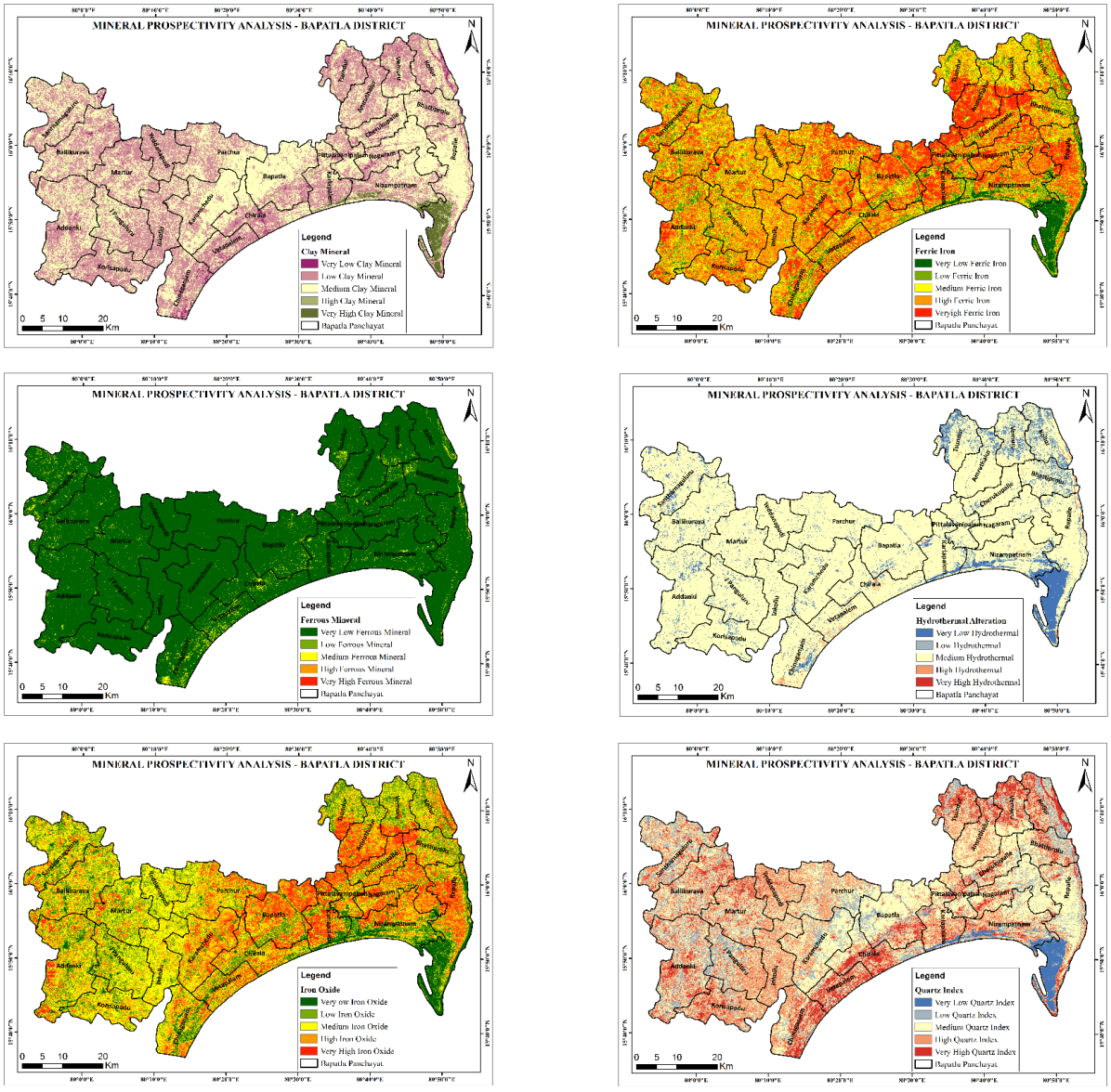


Fig. 5: Spectral Mineral Indices: Clay Mineral, Ferric Iron, Ferrous Mineral, Alteration-Related Index, Iron Oxide and Quartz Index.

3.3.3. Ferrous mineral

In contrast, the Ferrous Mineral map is dominated by Very Low concentrations, with only several scattered regions featuring Medium or Low contents. The absence of Ferrous Minerals in the majority of Bapatla district suggests that the area's iron geochemistry is primarily dominated by ferric compounds.

3.3.4. Alteration-related spectral index

The alteration-related spectral index map is overwhelmingly dominated by Medium alteration, with only a few High or Very High spots near Chinaganjam and the NE territories. Very Low levels (blue) occur sporadically in the central part of the district and form an extended area near Nizampatnam and Repalle, which likely reflects the presence of water bodies in these zones. On the other hand, Medium and High values (yellow–red) delineate several spectral anomaly zones in the NE, which require field and geochemical verification before being interpreted as hydrothermal alteration.

3.3.5. Iron oxide

Similar to the Ferric Iron distribution, Iron Oxide content is mostly High or Very High (orange-red) throughout the central and eastern territories (Bapatla, Parchur, Karamchedu, Chirala, Pittalavanipalem, Tsundur, Cherukupalle, Bhattiprolu, Repalle) with only scattered Low deposits near Parchur and the coastal edge of Nizampatnam and Repalle (dark green). Thus, the distribution pattern of Iron Oxide mirrors the abundance of Ferric Iron, which may reflect iron-rich or lateritic soils, but could equally reflect agricultural soil colour, moisture or sediment mineralogy; field and geochemical verification is required before any interpretation as iron-oxide mineralisation.

3.3.6. Quartz index

The Quartz Index map also demonstrates the area-wide presence of High or Very High concentrations (orange-red). Specifically, these include the western part (Addanki, Korisapadu, J Panguluru, Martur, Yeddanapudi, Santhamaguluru, Ballikurava) and NE provinces (Tsundur, Amruthalur, Vemuru, Cherukupalle), as well as the coastal strip with Vetapalem and Chinaganjam. Medium values (pale yellow) are found in the district's central part (Bapatla, Karlapalem), while the water body near Nizampatnam and Repalle is covered in Very Low deposits (blue). In general, the Quartz Index distribution reflects the pattern of lineament density and topographic complexity identified earlier, with maximum values in the NE and western parts of the district. High quartz-index values over the alluvial plain are more likely to reflect quartz-rich sands and silty soils than silicification; they are not evidence of quartz veining without field confirmation.

3.4. Surface indices

Surface indices (bare soil, moisture and vegetation) are used here as masks and indicators of quality: they indicate where a spectral mineral anomaly might be an artefact of vegetation, moisture or water, rather than an exposed-soil or rock response. Given that the district is predominantly cropland and irrigated land with coastal wetlands, much of the area was unsuitable for direct spectral mineral mapping. Pixels with high NDVI, high NDMI, or open water were therefore excluded prior to calculation of spectral mineral indices, and the maps below indicate where this masking has been applied.

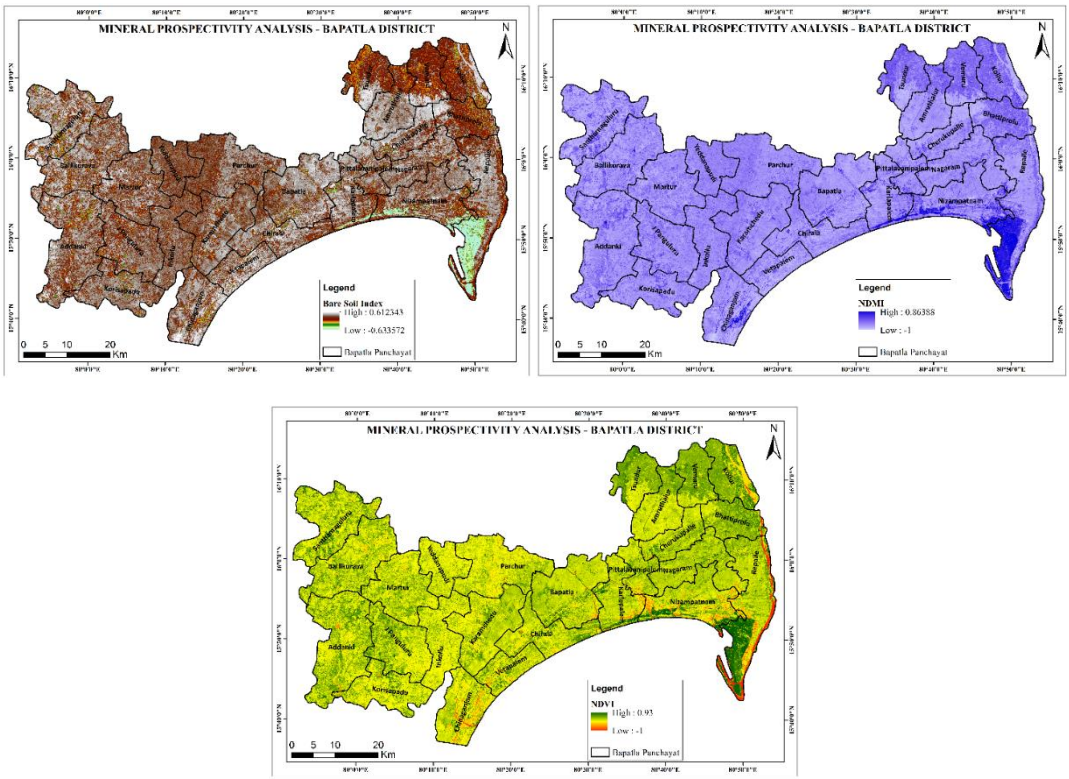


Fig. 6: Surface Indices: Bare Soil Index, NDMI and NDVI.

3.4.1. Bare soil index

The bare soil index map is generally dominated by High Bare Soil (dark brown to black) that dominates the central and western mandals of the district of Parchur, Yeddanapudi, Karamchedu, Martur, J Panguluru, Addanki, as well as the northern cluster of Tsundur, Amruthalur, Vemuru, and Kollur. This suggests that across most of the district, vegetation cover is typically low, and the spectral response of the area is likely to be dominated by bare soil or farmland, which has implications for the interpretation of the spectral mineralisation indices identified earlier; however, bare-soil exposure on cropland is seasonal (fallow or post-harvest fields) and does not make a spectral anomaly

mineralogical; an anomaly may reflect soil colour or tillage state. The only areas of the district that exhibit Low Bare Soil (light green) are the coastal region around Repalle and Nizampatnam, which are likely to be covered by water bodies and/or wetlands.

3.4.2. NDMI

The NDMI map is generally dominated by Moderate (light purple/lavender) and Low (pale lavender) classes that extend across most of the inland region of the district, which is consistent with the overall low levels of vegetation cover observed on the bare soil map. However, along the coastal region, especially around Nizampatnam and Repalle, the class shifts to High NDMI (dark blue-violet), which indicates the presence of water bodies and/or wetlands. Thus, overall, except for the coastal strip, most of the district is characterised by moderate to low soil moisture levels, which suggests lower moisture interference inland than near the coast; irrigated fields and canals can, however, raise soil moisture locally, so anomalies in cropped areas should also be treated with caution. However, spectral mineralisation anomalies observed near the coast should be treated with caution due to the potential effect of moisture on the spectral properties of surface rocks.

3.4.3. NDVI

The NDVI map is generally characterised by Medium vegetation vigour (yellow-green), which dominates the district's agricultural landscape. Healthy vegetation (dark green) is observed in patches along the coastal region, particularly in Bapatla, Karamchedu, Chirala, as well as the coastal strip around Nizampatnam and Repalle, which is likely to be caused by mangroves and/or riparian forests along the estuaries. Sparse vegetation (orange-red) is observed in patches around urban centres and along linear objects, such as roads. Thus, the overall vegetation cover in the district is moderate, with a mixture of agriculture-related vegetation, healthy vegetation along the coast, and vegetation-free patches in urban areas and along roads. Because agriculture dominates the district, vegetation and crop residue can still affect SWIR-based indices over large areas, so vegetated pixels were masked before index computation rather than assumed to have a negligible effect. However, the high vegetation vigour observed around Nizampatnam and Repalle, as well as along the estuaries, may interfere with spectral observations of surface minerals in these areas.

3.5. Mineral prospectivity

Mineral prospectivity mapping is the final stage in a mineral prospectivity study, where all themes identified in the study area are integrated into a weighted composite theme, showing the relative prospectivity of each area, ranging from Very Low to Very High. The index is a relative, knowledge-driven ranking of spectral and structural evidence and not a probability of mineral occurrence. The figure below shows the final composite theme for Bapatla district, which takes the form of a relatively fine mosaic. The overall impression is that of a landscape mostly dominated by areas of Very Low to Medium Mineral Prospectivity (green, olive and yellow), punctuated by relatively narrow, winding corridors of High to Very High Mineral Prospectivity (orange to red) running roughly north-west to south-east through the district, but most prominently through Santhamaguluru, Ballikurava, Yeddanapudi, Karamchedu, Bapatla, Karlapalem, Nizampatnam and Repalle. It follows the pattern of the drainage and lineament themes identified above, and shows that areas of structural control on mineral prospectivity tend to be relatively narrow corridors, rather than broader regions.

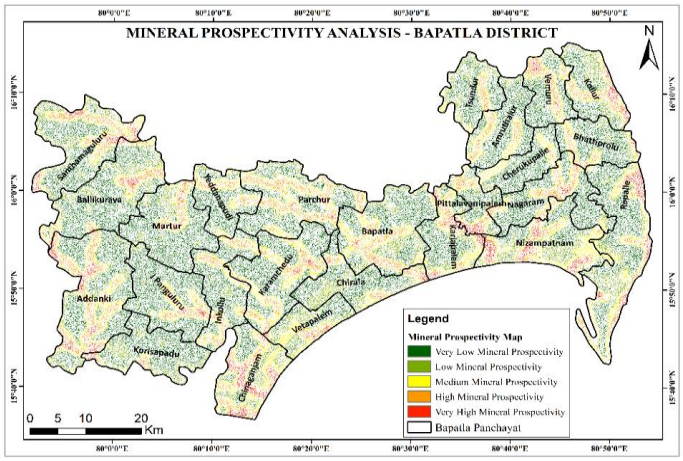


Fig. 7: Mineral Prospectivity Map of Bapatla District.

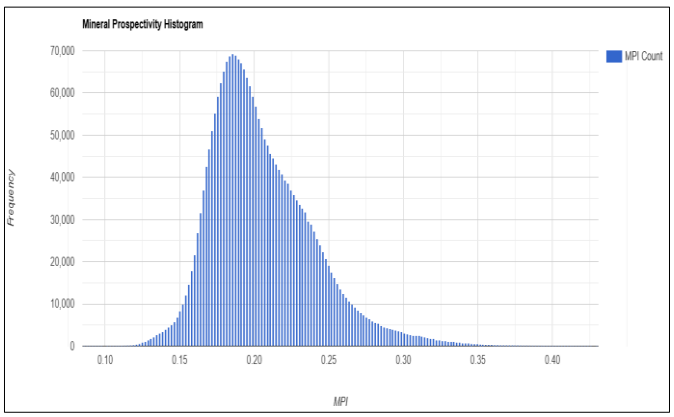


Fig. 8: Histogram of the Mineral Prospectivity Index (MPI) Values.

Table 4: Mandal-Wise Area (Km²) Under Each Mineral Prospectivity Class

Mineral Prospectivity								
Sl. No	Mandals	Very Low	Low	Medium	High	Very High	Area (Sq. Km.)	Area (%)
1	Addanki	237.46	97.65	75.19	114.70	33.51	279.28	7.17
2	Amruthalur	150.43	40.61	35.35	27.98	0.00	128.62	3.30
3	Ballikurava	248.79	120.92	34.25	43.55	10.72	223.38	5.74
4	Bapatla	191.13	122.41	67.69	63.44	3.69	218.27	5.61
5	Bhattiprolu	127.76	37.82	22.21	22.64	0.91	104.60	2.69
6	Cherukupalle	131.83	28.71	31.38	5.92	0.00	94.84	2.44
7	Chinaganjam	44.65	90.87	69.98	66.85	45.55	151.67	3.90
8	Chirala	148.18	99.61	26.69	22.70	4.50	140.58	3.61
9	Inkollu	154.11	45.00	45.21	49.52	0.04	146.33	3.76
10	J Panguluru	238.04	44.78	29.70	31.07	5.10	170.03	4.37
11	Karamchedu	225.42	49.96	80.44	53.14	4.64	204.99	5.27
12	Karlapalem	103.81	56.56	48.20	38.82	18.71	124.02	3.19
13	Kollur	82.00	82.13	25.79	36.37	14.81	117.25	3.01
14	Korisapadu	183.02	87.25	9.41	8.44	4.42	144.89	3.72
15	Martur	247.16	66.61	19.41	33.69	2.58	180.71	4.64
16	Nagaram	202.72	33.19	35.59	50.72	6.53	114.17	2.93
17	Nizampatnam	86.78	116.64	95.88	55.86	42.69	184.11	4.73
18	Parchur	161.34	80.55	76.50	95.94	4.03	212.08	5.45
19	Pittalavanipalem	54.29	39.11	23.17	22.05	17.03	71.58	1.84
20	Repalle	222.29	129.36	88.61	59.44	31.61	268.15	6.89
21	Santhamaguluru	167.22	111.20	49.00	73.92	19.17	209.06	5.37
22	Tsundur	105.48	73.86	20.19	15.84	0.00	105.68	2.71
23	Vemuru	102.79	31.99	29.17	38.05	6.97	101.40	2.60
24	Vetapalem	56.69	83.03	39.06	19.53	4.62	91.95	2.36
25	Yeddanapudi	117.09	36.82	29.89	27.83	0.00	105.52	2.71
Total							3893.13	100

The Mandal-wise information presented in Table 4 confirms the visual impression derived from Figure 7 regarding the distribution of prospectivity classes across the district's mandals. About overall area size, the five largest mandals are Addanki (7.17%), Repalle (6.89%), Ballikurava (5.74%), Bapatla (5.61%), and Parchur (5.45%), which possess, in addition to large acreage of High-to-Very High prospectivity (Addanki accounting for the largest combined High + Very High acreage of any mandal with 114.70 + 33.51 = 148.21 sq.km), significant High (Parchur: 95.94 sq.km) and Very High prospectivity (Chinaganjam: 45.55 sq.km of Very High, the largest such value across the district) areas, respectively. The two coastal mandals of Nizampatnam (42.69 sq.km of Very High prospectivity) and Repalle (31.61 sq.km of Very High prospectivity) also possess considerable High-to-Very High acreage, despite the generally low relief of the region, which suggests that lineament-, drainage-, and mineral (quartz, iron oxide)-controlled prospectivity may have more impact on exploration prioritisation than topography in this area. In contrast, the area of Very High prospectivity for Cherukupalle, Amruthalur, Tsundur, and Yeddanapudi is either non-existent or relatively small, compared to other mandals. Thus, the zones that may merit follow-up, subject to field verification, are the Addanki-Martur-Ballikurava triangle in the northwest part of the district, the Parchur-Karamchedu-Bapatla triangle in the centre, and the coastal Chinaganjam-Nizampatnam-Repalle triangle in the southeast, which possess the largest areas of High and Very High prospectivity, reflecting the findings of the analysis of individual thematic layers.

3.6. Principal component analysis

Principal component analysis of the six Sentinel-2 bands yields six components; the explained variances are shown in Fig. 9. Since the principal components are orthogonal by construction, the lack of correlation between them (−0.2 to 0.22, Fig. 11) is not surprising and does not imply that any particular component is geologically irrelevant; on the contrary, for scores calculated on the same pixels as the eigenvectors, correlations should be exactly zero, so that the reported nonzero values probably reflect a calculation on a different subset of the data. The scatter and box plots suggest one large cluster with outliers. PC4 has a group of low outliers at around −3 in PC1–PC3 space (Fig. 9), which should be mapped and checked against water, cloud shadows, built-up areas, and bright fields before interpreting PC4 as an alteration-related component. PC4 should only be considered an alteration-sensitive vector if the loadings match the diagnostic patterns; otherwise, it reflects noise or land cover variability and should not be considered as evidence of argillic alteration.

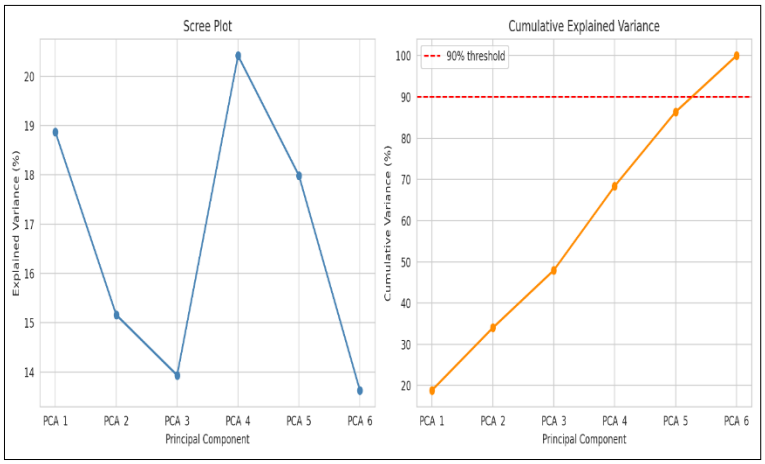


Fig. 9: Scree Plot and Cumulative Explained Variance Across the Six Principal Components.

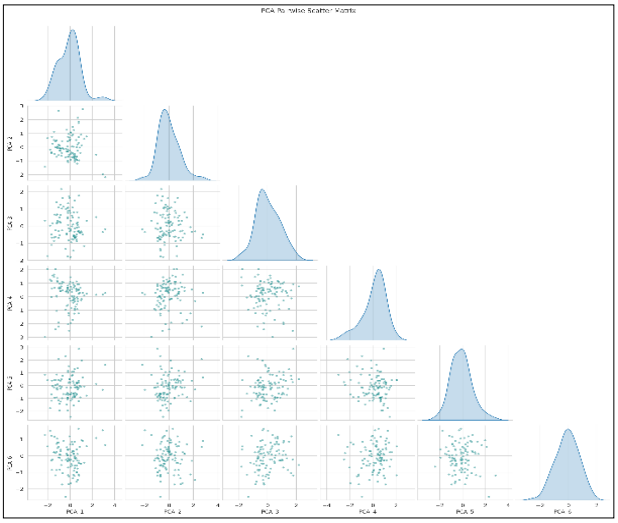


Fig. 10: Pairwise Scatter Matrix of All Six.

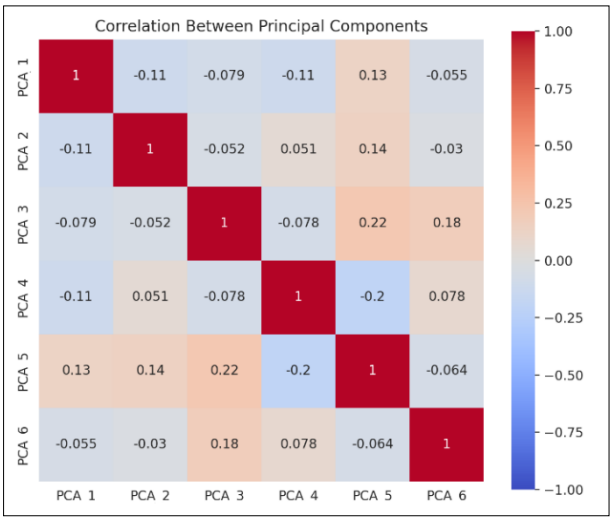


Fig. 11: Correlation Matrix (Orthogonality).

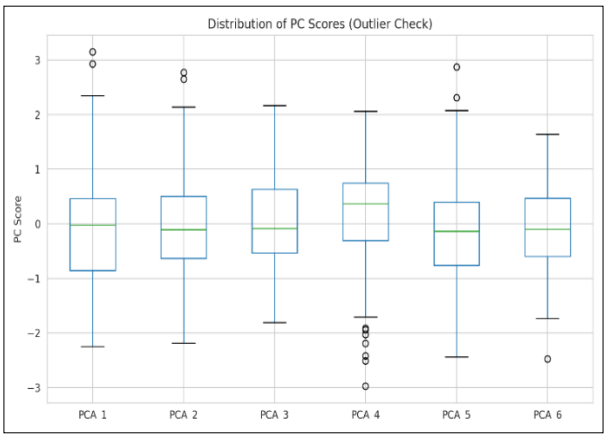


Fig. 12: Boxplots of PC notably PC4.

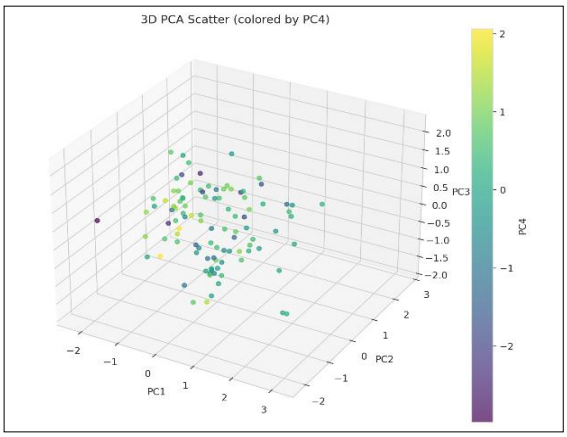


Fig. 13: 3D Scatter Plot.

3.7. Validation

The Prospectivity map was compared to a mineral occurrence layer from NGDR/GSI. The occurrence layer was not used to determine the AHP weights, and none of the eight MPI layers were derived from it. The comparison is not entirely independent if the lineament layer comes from Bhuvan/GSI products, or if the occurrence map is a density surface derived from the same structural layers, acknowledging this limitation. Comparison shows that the Mineral Occurrence map has significantly higher density of High to Very High classes (orange-red) that occupy large areal extents in most of the western and central belt mandals - Santhamaguluru, Ballikurava, Martur, Yeddanapudi, J Panguluru, Korisapadu, Karamchedu, Inkollu, as well as the northeast mandals of Tsundur, Amruthalur, Vemuru, while the Mineral Prospectivity map is much more conservative, only exhibiting High-Very High classes as narrow elongated corridors within the overall low-to-very low matrix.

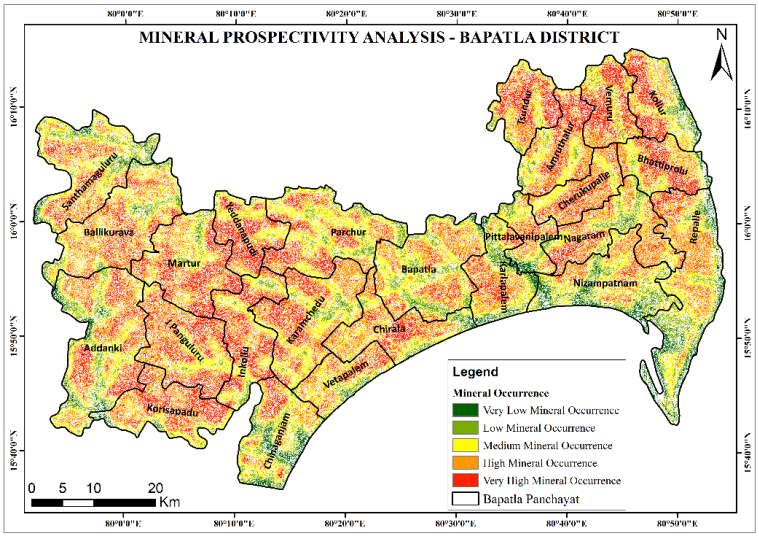


Fig. 14: Mineral Occurrence Map Used for Comparison.

However, the two maps do broadly agree with each other at the level of individual mandals, as the same areas - Santhamaguluru/Ballikurava (NW), Yeddanapudi/Karamchedu/Bapatla (central) and Karlapalem-Nizampatnam-Repalle corridor (eastern) - are reflected as High or Very High in the prospectivity map, albeit more conservatively, channelized along certain structural zones rather than exhibited as large-scale areal expanses as in the case of the Mineral Occurrence map; this indicates broad spatial correspondence only; a visual map-to-map comparison cannot quantify the hit rate and does not demonstrate predictive power.

4. Conclusion

The integrated mineral prospectivity analysis of Bapatla District suggests that despite the prevailing low-relief coastal and deltaic setting, it is possible to identify spatial patterns of spectral and structural anomalies that may be relevant to mineral potential through an appropriate combination of the considered terrain, structural, spectral, and surface condition attributes. The analysis of terrain characteristics (Relief, Slope, Topographic Positioning Index) indicated that the study area is largely a featureless coastal plain, with the only relatively high relief located in the northwest of the district (Santhamaguluru Ballikurava Martur belt). This observation was supported and expanded upon by the analysis of structural features – Drainage Density and Lineament Density, which highlighted the same north-western structural peculiarity and additionally identified a northeast structural trend near the Krishna delta boundary (Tsundur, Amruthalur, Vemuru, Kollur, Cherukupalle, Bhattiprolu) as areas of possible mineralisation foci associated with enhanced fracture development and favourable flow paths for mineral-bearing solutions.

The Analysis of spectral mineral composition highlighted the widespread occurrence of ferric iron, iron oxide, and quartz in the western and northeastern parts of the district, with overall moderate values of the clay mineral and alteration-related spectral indices. These observations were consistent with the structural trends identified in the study, with the exception of a few coastal localities (Repalle, Chinaganjam) characterised by high values of the clay mineral and alteration-related spectral indices. Bare soil, NDMI, and NDVI were used to mask vegetated and moist pixels; in the remaining pixels, the spectral indices are more likely to reflect surface mineralogy, although soil colour, tillage, and irrigation effects cannot be excluded. Thus, the findings related to the prevalence of ferric iron, iron oxide, and quartz were not contradicted by the survey of surface conditions, which identified them as being widespread, but concentrated in the lowland coastal areas of the district. At the same time, the identified association of ferric iron with clay minerals and hydrothermal alteration in the coastal zone, as well as the overall spectral similarity between these materials, appeared to be less certain due to the relatively high content of vegetation and surface moisture in these areas.

Overall, the integration of the findings related to high drainage density, lineament density, and the prevalence of ferric iron, iron oxide, and quartz produced relatively widespread, but narrow bands of High-to-Very High prospectivity in the north-western (Addanki–Ballikurava–Martur), central (Parchur–Karamchedu–Bapatla) and southeast (Chinaganjam–Nizampatnam–Repalle) parts of the district, which corresponded to the major structural trends observed in the study. These patterns were generally consistent with the mandal-level statistics, with Addanki, Parchur, and Chinaganjam being identified as the major contributors in terms of both High and Very High prospectivity areas. In turn, the areas of low mineral prospectivity (mostly Cherukupalle, Amruthalur, Tsundur, and Yeddanapudi mandals) showed almost no high-prospectivity zones. Thus, the final prospectivity map revealed three prospective areas that could be prioritised for ground follow-up surveys and geochemical sampling. This map demonstrates the most promising spectral-structural targets for mineral exploration. Nevertheless, the findings should be used with caution due to several limitations of the study.

Firstly, the target mineral system for the study was not defined. The analysis only explored the possibility of mineralization in the region, not the specific type of mineralization. Secondly, the study area is mostly covered by Quaternary sediments and consists of a large agricultural region. Thus, the detected spectral anomalies might represent different soil types, agricultural activities, or hydrological features. Thirdly, the weights used in the AHP might be biased, as they were based on expert judgments only. Lastly, there was no independent validation of the obtained results, and the accuracy of the findings is closely linked to the accuracy of the mineral occurrence map. Therefore, field geochemical surveys and verification tests are required before using the results for further exploration activities.

Acknowledgement

The authors sincerely acknowledge the Department of Geography, Kannur University, Kannur, for providing the academic support and facilities necessary to conduct this study. The authors gratefully acknowledge the European Space Agency (ESA) and Copernicus Programme for providing Sentinel-2A MSI Level-2 and Sentinel-1 GRD satellite data used for spectral mineral indices, vegetation and moisture analysis, and lineament and structural interpretation. The authors also thank the Bhuvan Portal, ISRO, for providing Carto-DEM data used for terrain, slope, relief, topographic position index, stream extraction, and drainage density analysis. We acknowledge the ASTER data providers for thermal and hydrothermal mapping and the National Geospatial Data Repository (NGDR) for geological datasets. The authors further acknowledge the Geological Survey of India (GSI) for lithological information and the National Bureau of Soil Survey and Land Use Planning (NBSS & LUP) for soil data. The Google Earth Engine (GEE) cloud-computing platform is gratefully acknowledged for facilitating large-scale geospatial data processing, analysis, and export. The authors express their sincere gratitude to all institutions and data providers for making these resources available for scientific research.

References

[1] Abdullah, A., Akhir, J. M., & Abdullah, I. (2010). Automatic mapping of lineaments using shaded relief images derived from digital elevation models (DEMs) in the Maran–Sungi Lembing area, Malaysia. Electronic Journal of Geotechnical Engineering, 15(J), 1–9, https://api.semanticscholar.org/CorpusID:135241374.

[2] Abrams, M. (2000). The Advanced Spaceborne Thermal Emission and Reflection Radiometer (ASTER): Data products for the high spatial resolution imager on NASA's Terra platform. International Journal of Remote Sensing, 21(5), 847–859. https://doi.org/10.1080/014311600210326.

[3] Abrams, M., Ashley, R., Rowan, L., Goetz, A., & Kahle, A. (1977). Mapping of hydrothermal alteration in the Cuprite mining district, Nevada, using aircraft scanner images for the spectral region 0.46 to 2.36 μm. Geology, 5(12), 713–718. https://doi.org/10.1130/0091-7613(1977)5<713:MOHAIT>2.0.CO;2.

[4] Arulbalaji, P., Padmalal, D., & Sreelash, K. (2019). GIS and AHP Techniques-Based Delineation of Groundwater Potential Zones: A case study from Southern Western Ghats, India. Sci Rep 9, 2082 (2019). https://doi.org/10.1038/s41598-019-38567-x.

[5] Behera, S., Panigrahi, M. K., & Pradhan, A. (2019). Identification of geochemical anomaly and gold potential mapping in the Sonakhan Greenstone belt, Central India: An integrated concentration-area fractal and fuzzy AHP approach. Applied Geochemistry, 107, 45-57. https://doi.org/10.1016/j.apgeochem.2019.05.015.

[6] Behnia, P., Harris, J. R., Rainbird, R. H., Williamson, M. C., & Sheshpari, M. (2012). Remote predictive mapping of bedrock geology using image classification of Landsat and SPOT data, western Minto Inlier, Victoria Island, Northwest Territories, Canada. International journal of remote sensing, 33(21), 6876-6903. https://ostrnrcan-dostrncan.canada.ca/handle/1845/155942. https://doi.org/10.1080/01431161.2012.693219.

[7] Benaissi, L., Tarek, A., Tobi, A., Ibouh, H., Zaid, K., Elamari, K., & Hibti, M. (2022). Geological mapping and mining prospecting in the Aouli inlier (Eastern Meseta, Morocco) based on remote sensing and geographic information systems (GIS). China Geology, 5(4), 614–625. https://doi.org/10.31035/cg2022035.

[8] Bhatta, B. (2008). Remote sensing and GIS. Oxford University Press.

[9] Bonham-Carter, G. F. (1994). Geographic information systems for geoscientists: Modelling with GIS. Pergamon.

[10] Bonham-Carter, G. F., Agterberg, F. P., & Wright, D. F. (1989). Integration of geological datasets for gold exploration in Nova Scotia. Digital geologic and geographic information systems, 10, 15-23. https://doi.org/10.1029/SC010p0015.

[11] Carranza, E. J. M. (2008). Geochemical anomaly and mineral prospectivity mapping in GIS (Handbook of Exploration and Environmental Geochemistry, Vol. 11). Elsevier.

[12] Carranza, E. J. M., & Hale, M. (2001). Geologically constrained fuzzy mapping of gold mineralisation potential, Baguio district, Philippines. Natural Resources Research, 10(2), 125-136. https://doi.org/10.1023/A:1011500826411.

[13] Carranza, E. J. M., & Hale, M. (2002). Mineral imaging with LANDSAT thematic mapper data for hydrothermal alteration mapping in heavily vegetated terrane. International journal of remote sensing, 23(22), 4827-4852. https://doi.org/10.1080/01431160110115014.

[14] Carranza, E. J. M., Sadeghi, M., & Billay, A. (2015). Predictive mapping of prospectivity for orogenic gold, Giyani greenstone belt (South Africa). Ore Geology Reviews, 71, 703–718. https://doi.org/10.1016/j.oregeorev.2014.10.030.

[15] Chang, D. Y. (1996). Applications of the extent analysis method on fuzzy AHP. European Journal of Operational Research, 95(3), 649–655. https://doi.org/10.1016/0377-2217(95)00300-2.

[16] Crosta, A. P., De Souza Filho, C. R., Azevedo, F., & Brodie, C. (2003). Targeting key alteration minerals in epithermal deposits in Patagonia, Argentina, using ASTER imagery and principal component analysis. International Journal of Remote Sensing, 24(21), 4233–4240. https://doi.org/10.1080/0143116031000152291.

[17] Crosta, A. P., & Moore, J. M. (1989). Enhancement of Landsat Thematic Mapper imagery for residual soil mapping in SW Minas Gerais State, Brazil: A prospecting case history in greenstone belt terrain. In Proceedings of the 7th ERIM Thematic Conference: Remote Sensing for Exploration Geology (pp. 1173–1187). Environmental Research Institute of Michigan.

[18] Fu, Y., Cheng, Q., Jing, L., Ye, B., & Fu, H. (2023). Mineral Prospectivity Mapping of Porphyry Copper Deposits Based on Remote Sensing Imagery and Geochemical Data in the Duolong Ore District, Tibet. Remote Sensing, 15(2), 439. https://doi.org/10.3390/rs15020439.

[19] Gad S, & Kusky T. (2006) Lithological mapping in the Eastern Desert of Egypt, the Barramiya area, using Landsat thematic mapper (TM) Journal of African Earth Sciences, 44 (2) 196-202 https://doi.org/10.1016/j.jafrearsci.2005.10.014.

[20] Guo, Y., Zhang, S., Fu, C., & Yang, Y. (2023). GIS-based mineral prospectivity mapping: a systematic study on machine learning at Hezuo-Meiwu District, Gansu Province", Proc. SPIE 12552, International Conference on Geographic Information and Remote Sensing Technology (GIRST 2022), 125523A (10 Feb 2023); https://doi.org/10.1117/12.2667272.

[21] Gupta, R. P. (2003). Remote sensing geology (2nd ed.). Springer. https://doi.org/10.1007/978-3-662-05283-9.

[22] Hajaj, S., El Harti, A., Pour, A. B., Jellouli, A., Adiri, Z., & Hashim, M. (2024). A review on hyperspectral imagery application for lithological mapping and mineral prospecting: Machine learning techniques and future prospects. Remote Sensing Applications: Society and Environment, 35, 101218. https://doi.org/10.1016/j.rsase.2024.101218.

[23] Hung, L. Q., Batelaan, O., & De Smedt, F. (2005, October). Lineament extraction and analysis, comparison of LANDSAT ETM and ASTER imagery. Case study: Suoimuoi tropical karst catchment, Vietnam. In Remote sensing for environmental monitoring, GIS applications, and geology V (Vol. 5983, pp. 182-193). SPIE. https://doi.org/10.1117/12.627699.

[24] Loughlin, W. P. (1991). Principal component analysis for alteration mapping. Photogrammetric Engineering and Remote Sensing, 57(9), 1163–1169.

[25] Maleki, M., Niroomand, S., Farahbakhsh, E., Modabberi, S., & Tajeddin, H. A. (2021). Hydrothermal alteration and structural mapping of the Qolqoleh-Kasnazan shear zone in Iran using remote sensing data. Arabian Journal of Geosciences, 14(16), 1576. https://doi.org/10.1007/s12517-021-07920-8.

[26] Manyoe, I. N., & Hutagalung, R. (2021). Application of lineament density extraction based on digital elevation model for geological structures control analysis in Suwawa geothermal area. Journal of Geoscience, Engineering, Environment, and Technology, 6(3), 141–148. https://doi.org/10.25299/jgeet.2022.7.3.8085.

[27] McCuaig, T. Campbell, Steve Beresford, and Jon Hronsky. (2010). Translating the mineral systems approach into an effective exploration targeting system. Ore Geology Reviews 38: 128–138. https://doi.org/10.1016/j.oregeorev.2010.05.008.

[28] Ninomiya, Y., Fu, B., & Cudahy, T. J. (2005). Detecting lithology with Advanced Spaceborne Thermal Emission and Reflection Radiometer (ASTER) multispectral thermal infrared "radiance-at-sensor" data. Remote Sensing of Environment, 99(1–2), 127–139. https://doi.org/10.1016/j.rse.2005.06.009.

[29] Nugroho, U. C., & Tjahjaningsih, A. (2016). Lineament density information extraction using DEM SRTM data to predict the mineral potential zones. International Journal of Remote Sensing and Earth Sciences, 13(1), 55–64. https://doi.org/10.30536/j.ijreses.2016.v13.a2704.

[30] Rowan, L. C., Hook, S. J., Abrams, M. J., & Mars, J. C. (2003). Mapping hydrothermally altered rocks at Cuprite, Nevada, using the Advanced Spaceborne Thermal Emission and Reflection Radiometer (ASTER), a new satellite-imaging system. Economic Geology, 98(5), 1019–1027. https://doi.org/10.2113/gsecongeo.98.5.1019.

[31] Saaty, T. L. (1980). The analytic hierarchy process: Planning, priority setting, resource allocation. McGraw-Hill.

[32] Sabins, F. F. (1999). Remote sensing for mineral exploration. Ore Geology Reviews, 14(3–4), 157–183. https://doi.org/10.1016/S0169-1368(99)00007-4.

[33] Tangestani, M. H., & Moore, F. (2002). Porphyry copper alteration mapping at the Meiduk area, Iran. International Journal of Remote Sensing, 23(22), 4815–4825. https://doi.org/10.1080/01431160110115564.

[34] Van der Meer, F. D., Van der Werff, H. M., Van Ruitenbeek, F. J., Hecker, C. A., Bakker, W. H., Noomen, M. F., Van Der Meijde, M., Carranza, E. J. M., De Smeth, J. B., & Woldai, T. (2012). Multi- and hyperspectral geologic remote sensing: A review. International Journal of Applied Earth Observation and Geoinformation, 14(1), 112–128. https://doi.org/10.1016/j.jag.2011.08.002.

[35] Yamaguchi, Y., & Naito, C. (2003). Spectral indices for lithologic discrimination and mapping by using the ASTER SWIR bands. International Journal of Remote Sensing, 24(22), 4311–4323. https://doi.org/10.1080/01431160110070320.

[36] Yousefi, M., Carranza, E. J. M., Kreuzer, O. P., Nykänen, V., Hronsky, J. M., & Mihalasky, M. J. (2021). Data analysis methods for prospectivity modelling as applied to mineral exploration targeting: State-of-the-art and outlook. Journal of Geochemical Exploration, 229, Article 106839. https://doi.org/10.1016/j.gexplo.2021.106839.

[37] Fawcett, T. (2006). An introduction to ROC analysis. Pattern Recognition Letters, 27(8), 861–874. https://doi.org/10.1016/j.patrec.2005.10.010.

[38] Yousefi, M., & Carranza, E. J. M. (2015). Prediction–area (P–A) plot and C–A fractal analysis to classify and evaluate evidential maps for mineral prospectivity modeling. Computers & Geosciences, 79, 69–81. https://doi.org/10.1016/j.cageo.2015.03.007.